LUND UNIVERSITY

Thermodynamic Assessment of the As-Zn and As-Ga-Zn Systems

Ghasemi, Masoomeh; Johansson, Jonas

Thermodynamic Assessment of the As-Zn and As-Ga-Zn Systems

Masoomeh Ghasemi[a,*], Jonas Johansson[a]

[a]*Solid State Physics, Lund University, Box 118 SE-22100 Lund, Sweden*

Abstract

We have performed a thermodynamic assessment of the As-Zn and As-Ga-Zn systems. The systems are assessed based on the CALPHAD method and using available first principles and experimental data. Using the optimized set of parameters found in this work, the calculated As-Zn binary phase diagram, isoplethal sections and the monovariants lines of the As-Ga-Zn ternary system are presented. The comparison of the calculated diagrams with the experimental and first principles data shows good agreement.

Keywords: Phase diagrams, CALPHAD, Thermodynamic modeling.

1. Introduction

III-V semiconductors have attracted considerable attention due to their applications in fabrication of electronic and opto-electronic devices such as light emitting diodes and solar cells. The electrical properties of these semiconductors can be tuned by adding impurity atoms. Zinc is a common p-type dopant in the III-V semiconductor GaAs. It can be incorporated in GaAs either by adding it to the gas phase during the Metal-Organic Chemical Vapor Deposition (MOCVD) growth or after the growth via diffusion [1]. The knowledge of the phase equilibria of the As-Ga-Zn system can be of importance to understand the doping mechanisms during growth of Zn-doped GaAs.

The phase equilibria of this ternary system have been investigated in several studies [2, 3, 4, 5, 6]. The liquidus isotherms have been calculated using the regular solution model by Panish [3] and by Jordan [7]. However, there has been no CALPHAD modeling [8] of this ternary system. In this work we have assessed the phase diagram of the As-Ga-Zn system based on the CALPHAD technique using the available experimental data.

To assess a ternary system within this methodology, one requires the description of the binary sub-systems. We used the thermodynamic description of the As-Ga and Ga-Zn systems assessed by Ansara et al. [9] and Dutkiewicz et al. [10], respectively. Because the thermodynamic description of the As-Zn binary system was lacking in the literature, this system was also assessed in the present work.

The structure of the present manuscript is as following. First, available literature data on the As-Ga, Ga-Zn and As-Zn binary systems and the As-Ga-Zn ternary system are discussed. Next, the choice of thermodynamic models adapted for the existing phases in the As-Ga-Zn system will be motivated. Finally, the

calculated phase diagram of the As-Zn binary system and isoplethal sections and liquidus projection of the As-Ga-Zn ternary system will be presented and compared to the literature data.

2. Literature data

2.1. Binary systems

As-Ga:. In the As-Ga system, there are three solution phases, liquid, (Ga) and (As) and one stoichiometric phase, GaAs, with zinc-blende structure which melts congruently at 1510 K. There is a eutectic reaction at 1067 K and about 5.0 at.% Ga and a degenerate invariant reaction at 303 K and 100 at.% Ga. The system was assessed based on the CALPHAD method by Chatillon et al. [11]. They used the available phase diagram and thermochemical data for the assessment and proposed three sets of optimized parameters to calculate the phase diagram. The Ga-rich side of the phase diagram was satisfactorily reproduced using all parameter combinations. But, the parameter set which resulted in the most satisfactory fit in the As-rich side of the phase diagram with the least number of optimized coefficients was recommended. Later, this parameter set was reported by Ansara et al. [9] in the development of a consistent database for III-V binary compound semiconductor systems. The calculated As-Ga phase diagram using the recommended parameter set is shown in Fig 1-a.

Ga-Zn:. This binary system is a simple eutectic system consisting of three solution phases: liquid, hcp and (Ga). The eutectic reaction occurs at 298 K and about 4.0 at.% Zn. In the present work the parameters optimized by Dutkiewicz et al. [10] are used. The calculated Ga-Zn binary phase diagram is shown in Fig. 1-b.

As-Zn:. Okamoto summarized most of the available experimental measurements on the As-Zn system and constructed the phase diagram based on these data [12]. There are two stoichiometric phases in the As-Zn binary system. Both these stoichiometric phases, As_2Zn and As_2Zn_3, melt congruently; at 1043

and 1288 K, respectively. The As_2Zn phase has a narrow homogeneity range. The homogeneity range of the As_2Zn phase was determined by Lazarev et al. [13] to be between 33.0 and 33.5 at. % Zn.

Heike [14] assessed the system over the whole composition range using thermal and microscopic analyses. There are three eutectic reactions in this system at compositions of 21.0, 41.0 and ~ 99.8 at.% Zn and at 996, 1023 and 692 K, respectively. The As_2Zn_3 phase undergoes two polymorphic transformations; β-As_2Zn_3 $\leftrightarrow$ α'-As_2Zn_3 at 924 K and α'-As_2Zn_3 $\leftrightarrow$ α-As_2Zn_3 at 463 K (according to Okamoto [12] and based on Ref. [14]). Greenberg et al. [15] studied the $\beta \leftrightarrow \alpha'$ reaction by means of static vapor pressure measurements and declared that it occurs in the temperature range of 937 to 948 K. They also pointed out that the transition is incongruent with the composition change of 0.01 at.% towards the As-rich side.

Lazarev et al. [16] also performed differential thermal analysis on this system. Their measured liquidus temperatures at low concentrations of As (at about 12 and 20 at.% As) are considerably higher than the registered temperatures by Heike [14]. However, at higher concentrations of As, the agreement with Heike [14] is acceptable.

Friedrich and Leroux [17] measured the system at high compositions of Zn (89.4 to 99.5 at. % Zn). The determined eutectic temperature by Friedrich and Leroux close to the Zn corner agrees very well with that of Heike [14] but the liquidus temperatures are substantially higher.

In the most recent study of the thermodynamics of the As-Zn system, Yamaguchi et al. [18] measured the heat content of the liquid phase by drop calorimetry at the concentration range of 52.0 to 96.0 at. % Zn and the temperature range of 800 to 1450 K. They determined the liquidus temperatures for this composition range as the deflections of the heat content curves. Unfortunately, the heat content data are not tabulated which made it impossible to use them. However, the authors suggested the possible presence of the associates in the liquid phase based on the V-shaped enthalpy of mixing which was calculated from the heat content data.

Lyons [19] measured the dissociation pressure of As_2Zn in the range of 885 to 1043 K by means of the dew-point and the triple-point methods. The author extrapolated the melting point of the compound to be 1041 K at As pressure of 3.3 atm. Schoonmaker and Hemmerman [20] studied the vaporization of As_2Zn_3 using the torsion effusion method. They discussed that As_2Zn_3 sublimates congruently.

There is no experimental data (to the best of our knowledge) on the temperature dependency of the heat capacity of compounds. The calculated enthalpy of formation of the As_2Zn and As_2Zn_3 phases using first principles [21] is used for the assessment.

2.2. Ternary System

The As-Ga-Zn ternary system has been measured in several studies. Köster and Ulrich [2] investigated three isoplethal sections GaAs-Zn, GaAs-As_2Zn and GaAs-As_2Zn_3 (see Fig. 4). Based on their differential thermal analysis and X-ray diffrac-

tion results, they suggested that all these vertical sections are quasi-binary.

In a later study, Panish [3] measured the GaAs-Zn cut of the ternary phase diagram. The X-ray diffraction measurements showed that three primary phase fields, GaAs, As_2Zn_3 and Zn will be precipitated on cooling along the GaAs-Zn cut. It was suggested that the presence of the As_2Zn_3 phase has not been observed by Köster and Ulrich [2] in samples with high concentration of GaAs due to the small sizes of their samples. Panish also determined the liquidus and the phase transition temperatures using the differential thermal analysis. The temperatures were slightly lower than those measured by Köster and Ulrich [2]. In a separate study [4], Panish measured the GaAs-As_2Zn_3 cut of the phase diagram. It was in a good agreement with the results of Köster and Ulrich [2] except for in the vicinity of 1473 K. It was concluded that the error has been caused by the imposed thermal gradient (100 K hotter in the gas phase) by Köster and Ulrich [2] to prevent the condensation of arsenic. He calculated the liquidus curves using the regular solution model. He also determined the solid solubility of Zn in GaAs for 1000 °C isotherm to be 3.5×10^{20} at/cm^3 at the composition of 40.0 at.%Zn along the GaAs-Zn cut.

Pelevin et al. [6] performed differential thermal analysis and X-ray diffraction measurement on the compositions along the GaAs-Zn cut of the As-Ga-Zn phase diagram. In agreement with the results of Panish [3], they observed the presence of As_2Zn_3 for samples with compositions larger than 40.0 mol% GaAs. However, in the temperature range 883-918 K, they observed two thermal effects and associated those with the polymorphic transformation of As_2Zn_3, while only one thermal effect was observed by Panish [3].

Shih et al. [5] measured the partial pressure of As and Zn along the 900, 1000 and 1050 °C isotherms of the As-Ga-Zn phase diagram using an optical adsorption method. They determined the activity coefficients of the components which were found to be in agreement with the Gibbs-Duhem equations.

Tuck [22] calculated the solid solubility of Zn in GaAs at 1000 °C based on the experimental data and using the calculated concentration of point defects. It was concluded that the solubility of Zn in GaAs is less than 1.0 at.% which is equivalent to the maximum concentration of 3.8×10^{20} at/cm^3. Moreover, the deviation from the stoichiometry was calculated to be 0.0039 at.%As.

3. Gibbs Energy Models

In this section, the Gibbs energy models of the phases in the As-Ga-Zn system are described. The crystal structure of the solid phases and the adapted Gibbs energy model of all phases are summarized in Table.1.

3.1. Pure elements and stoichiometric phases

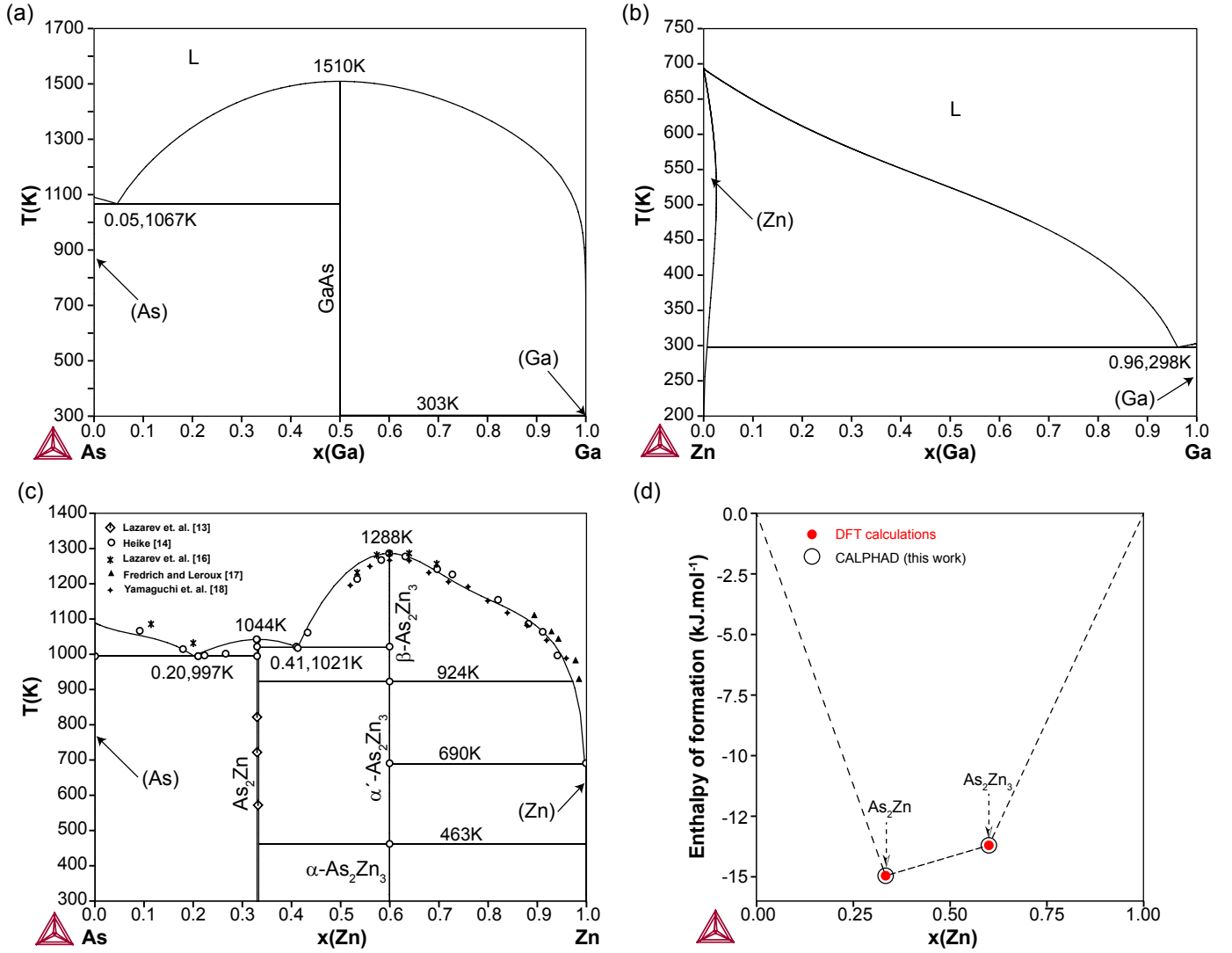The molar Gibbs energy, G_m, of an elemental phase θ is described by a function of temperature as:

Figure 1: (a) The calculated As-Ga binary phase digram using the parameters given in [9]. (b) The calculated Ga-Zn binary phase digram using the parameters optimized in [10]. (c) Calculated phase diagram of the As-Zn system using the optimized parameters in the present work. The experimental data points are superimposed on the diagram. (d) Calculated enthalpy of formation of compounds in the As-Zn system. The enthalpy values from first principles calculations [21] are marked on the plot (with red circles). The calculated enthalpies from the presents assessment are shown with hollow circles. The dashed line is only a guide to the eyes.

$$G_m^\theta - H^{\mathrm{SER}} = a_0 + a_1 T + a_2 T \ln(T) + a_3 T^2$$
$$+ a_4 T^{-1} + a_5 T^3 + ... \tag{1}$$

where H^{SER} is the enthalpy of the element in its reference state, i.e. its stable form at 298.15 K and 1 bar. The a_i coefficients are taken from the SGTE (Scientific Group Thermodata Europe) thermodynamic database [30] [1]. In Table 2, the Gibbs energies of pure elements used on the present assessment are listed.

The Gibbs energy of the stoichiometric phases will have the same form as Eq. 1 if heat capacity of the compound is mea-

sured as a function of temperature (ex. the GaAs phase). If there is no data on the heat capacity of the phase, as is the case for the As_2Zn_3 and As_2Zn phases, the heat capacity is the weighted average of the heat capacities of the end members. Hence, only a linear temperature dependency of the Gibbs energy of formation from the constituent elements was taken into account based on the Kopp-Neumann rule:

$$G_m^\theta = a_0 + a_1 T + \sum b_i G_i^\theta \tag{2}$$

where a_0 and a_1 are the coefficients to be optimized. The b_i coefficients are the stoichiometric ratios.

In the case of As_2Zn phase, the solubility of arsenic on the zinc sublattice is taken into account and the compound is modeled with a two-sublattice model as $(As)_2(As,Zn)$.

---

[1]The As-Ga and Ga-Zn binary systems have been assessed earlier than the updated SGTE database [30] but since the Gibbs energy descriptions of the pure elements of the present ternary system are unchanged, our calculated As-Ga and Ga-Zn binaries are consistent with the old assessments.

3

Table 1: Crystal structure, composition range and Gibbs energy models of all phases in the As-Ga-Zn ternary system.

| Phase	Prototype, struktur-bericht, Space group and Pearson symbol	Composition region	Model	Ref.
Liquid	-	-	(As,As$_2$Zn$_3$,Ga,Zn)	-
As-rhombohedral	α-As, *hR6*, 166, *R-3m*	As-Zn: 0 at.%Zn As-Ga: 0 at.%Ga	(As,Zn)	[23]
Ga-orthorhombic	Ga, *oS8*, 64, *Cmce*	As-Ga: 0 at.%As Ga-Zn: 0.8 at.%Zn	(Ga:Va)	[24]
Zn-hcp	Mg, *hP2*, 194, *P6$_3$/mmc*	As-Zn: 0 at.%As Ga-Zn: 2.36 at.%Ga	(As,Ga,Zn:Va)	[25]
GaAs	ZnS, *cF8*, 216, *F-43m*	50 at.%As	(Ga)(As)	[26]
As$_2$Zn	..., *mP24*, ..., *P2$_1$/c*	33.3-33.5 at.%Zn	(As)$_2$(As,Zn)	[27]
α'-As$_2$Zn$_3$	..., *tP40*, ..., *P4$_2$/nbc*	60 at.%Zn	(As)$_2$(Zn)$_3$	[28]
α-As$_2$Zn$_3$	..., *tI160*, ..., *I4$_1$cd*	60 at.%Zn	(As)$_2$(Zn)$_3$	[29]
β-As$_2$Zn$_3$	CaF$_2$, *cF12*, A3, *Fm-3m*	60 at.%Zn	(As)$_2$(Zn)$_3$	[29]
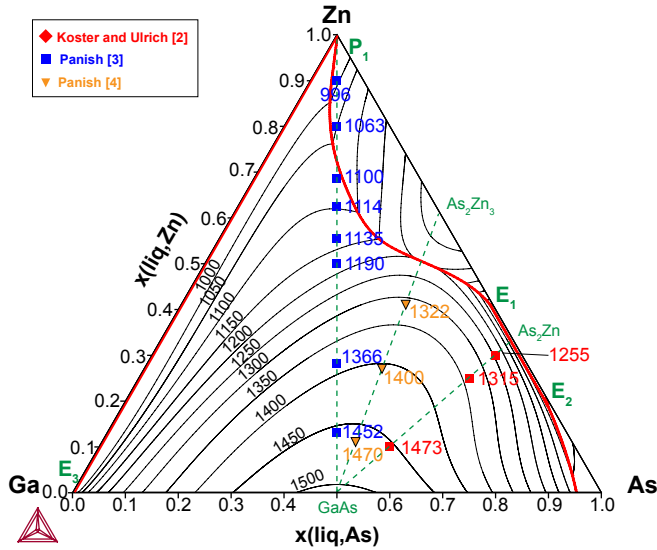
Figure 2: Calculated liquidus projection of the As-Ga-Zn ternary system with 50 K increment in temperature. The measured temperatures are superimposed on the diagram by symbols: diamond [2], square [3] and triangle [4]. The ternary invariant (eutectic 'E' and peritectic 'P') reactions are also marked.

3.2. Solution phases

In a solution phase all species are mixing on only one sublattice. There are four solution phases in the As-Ga-Zn system: liquid, (Ga), (As) and hcp. The Gibbs energy of a ternary solution phases is described by:

$$
\begin{aligned}
G^{\theta} = \sum_{m=i,j,k} y_m {}^0G_m^{\theta} + RT \sum_{m=i,j,k} y_m \ln(y_m) \\
+ \sum_i \sum_{j>i} y_i y_j L_{ij} + \sum_i \sum_{j>i} \sum_{k>j} y_i y_j y_k L_{ijk}
\end{aligned}
\tag{3}
$$

where the first term is the surface of reference, the second term is due to the configurational entropy and y_m is the site fraction of the phase constituents. The two last terms are the excess energy terms in which $L_{i,j}$ and $L_{i,j,k}$ are the binary and ternary interaction parameters, respectively. The composition dependence of the interaction parameters is expressed as:

$$
\begin{aligned}
L_{i,j} &= {}^0L_{ij} + (y_i - y_j) \cdot {}^1L_{ij} + (y_i - y_j)^2 \cdot {}^2L_{ij} \\
L_{i,j,k} &= y_i \cdot {}^0L_{ijk} + y_j \cdot {}^1L_{ijk} + y_k \cdot {}^2L_{ijk}
\end{aligned}
\tag{4}
$$

Unless there is data on the excess heat capacity, ${}^vL_{i,j}$ and ${}^vL_{i,j,k}$ are either temperature-independent or mostly only linearly dependent on the temperature.

There are two points that are to be discussed regarding the Gibbs energy models of the liquid and the hcp phases.

First, based on the heat content measurements of the liquid phase in the As-Zn system by Yamaguchi et al. [18], there is short range ordering in the liquid phase. It means that the liquid phase has a high tendency to form the molecules of the solid phase at the composition of the minimum enthalpy of mixing (at about 60 at.% Zn). Thus, the associate-solution model was adapted for the liquid phase: (As, As$_2$Zn$_3$, Zn) in the As-Zn binary system and correspondingly (As, As$_2$Zn$_3$, Ga, Zn) in the As-Ga-Zn ternary system with As$_2$Zn$_3$ as the associate.

Second, in some databases (e.g. COST 507 [31]), the Zn solid phase is modeled as HCP-ZN. Since zinc has an abnormal c/a ratio (1.86) with respect to the ideal ratio of the hexagonal close-packed structure (1.63), in the development of the mentioned database, it was assumed that a separate model should be used for this phase. However, Schmid-Fetzer and Hallstedt [32] recommended that this phase should be modeled as a hexagonal close-packed phase using the HCP-A3 model. Following their recommendation, in the current assessment the adapted model for the solid-Zn is HCP-A3.

Table 2: Gibbs energies of pure elements (in J/mole and K).

Element	Gibbs energies (J/moel)
As	Between 298.15 and 1090 K: ${}^0G_{As}^{SER} = -7270.447 + 122.211069\,T - 23.3144\,T\,\ln(T) - 0.00271613\,T^2 + 11600\,T^{-1}$ ${}^0G_{As}^{L} = 24442.9 - 22.424679\,T + {}^0G_{As}^{SER}$ ${}^0G_{As}^{hcp} = 24874 - 14\,T + {}^0G_{As}^{SER}$ Between 1090 and 1200 K: ${}^0G_{As}^{SER} = -10454.913 + 163.457433\,T - 29.216037\,T\,\ln(T)$ ${}^0G_{As}^{L} = 24442.9 - 22.424679\,T + {}^0G_{As}^{SER}$ ${}^0G_{As}^{hcp} = 24874 - 14\,T + {}^0G_{As}^{SER}$
Ga	Between 298.15 and 302.92 K: ${}^0G_{Ga}^{SER} = -21312.331 + 585.263691\,T - 108.228783\,T\,\ln(T) + 0.227155636\,T^2 - 1.18575257 \times 10^{-4}\,T^3 + 439954\,T^{-1}$ ${}^0G_{Ga}^{L} = 5491.31 - 18.073718\,T - 7.0154 \times 10^{-17}\,T^7 + {}^0G_{Ga}^{SER}$ ${}^0G_{Ga}^{hcp} = 4500 - 9.5\,T + {}^0G_{Ga}^{SER}$ Between 302.92 and 4000 K: ${}^0G_{Ga}^{SER} = -7055.643 + 132.73019\,T - 26.0692906\,T\,\ln(T) + 1.506 \times 10^{-4}\,T^2 - 4.0173 \times 10^{-8}\,T^3 - 118332\,T^{-1} + 1.645E+23\,T^{-9}$ ${}^0G_{Ga}^{L} = 5666.446 - 18.680788\,T - 1.64554 \times 10^{23}\,T^{-9} + {}^0G_{Ga}^{SER}$ ${}^0G_{Ga}^{hcp} = 4500 - 9.5\,T + {}^0G_{Ga}^{SER}$
Zn	Between 298.15 and 692.68 K: ${}^0G_{Zn}^{SER} = -4315.967 + 116.900389\,T - 23.701314\,T\,\ln(T) - 0.001712034\,T^2 - 1.264963 \times 10^{-6}\,T^3$ ${}^0G_{Zn}^{L} = +7157.213 - 10.29299\,T - 3.58958 \times 10^{-19}\,T^7 + {}^0G_{Zn}^{SER}$ ${}^0G_{Zn}^{rho} = -669.82 + 13.06968\,T + {}^0G_{Zn}^{SER}$ Between 692.68 and 1700 K: ${}^0G_{Zn}^{SER} = -8100.739 + 170.77598\,T - 31.38\,T\,\ln(T) + 4.70514 \times 10^{26}\,T^{-9}$ ${}^0G_{Zn}^{L} = +7450.123 - 10.736234\,T - 4.70657 \times 10^{26}\,T^{-9} + {}^0G_{Zn}^{SER}$ ${}^0G_{Zn}^{rho} = -669.82 + 13.06968\,T + {}^0G_{Zn}^{SER}$

4. Results and Discussion

The optimization of the parameters was carried out using the PARROT optimizer [33, 34, 35] of the Thermo-Calc software [36]. The Gibbs energy functions and the interaction parameters of all phases in the As-Ga-Zn system are summarized in Table 3.

As-Zn binary system:. The As-Zn system was assessed using the available experimental data of Heike [14], Yamaguchi et al. [18], Lazarev et al. [16], Friedrich and Leroux [17], Lazarev et al. [13] and Lyons [19].

The As-Zn binary phase diagram is calculated and compared to the experimental data in Fig. 1-c. There is a good agreement between the measured invariant, polymorphic transformation and congruent melting temperatures and compositions. Because the liquidus temperatures measured in different studies do not agree very well with each other, it was attempted to find the best fit to Ref. [14]. The optimization of the Gibbs energy model parameters is done using the least-square fitting. The optimizer tries to minimize the sum of the squares of the residuals (the difference between the calculated and the experimental values). Within this procedure, every piece of experimental data can be given a certain weight according to its reliability. The more reliable data is given a higher weight. Therefore, the weights of the experimental data were adjusted in a way that a higher weight was given to the data of [14], [18] and [16] which were in agreement with each other. The highest weight was given to the data set by Heike [14] and the lowest weigh was given to the data by Friedrich and Leroux [17].

Yamaguchi et al. [18] measured the heat content of liquid phase in the composition range of 52.0 to 96.0 at.% Zn but since the measured heat contents are not tabulated in the corresponding reference, only the reported liquidus temperatures (the deflections of the heat content curves) were used for the optimization. The determined temperatures by Yamaguchi et al. are lower than those reported by Heike [14] up to 20 K. Therefore, a lower weight was given to liquidus data of Yamaguchi at al.

Modeling the liquid phase using the associate model helped to fit to the liquidus temperatures but the minimum of the enthalpy of mixing occurs at higher As concentration when using our optimized parameters as compared to Yamaguchi's calculations [18] (See Fig. A.5). The authors believe that the liquid phase should be further optimized and this requires experimental data on the mixing characteristics.

Fig. 1-d shows the calculated enthalpy of formation of stoichiometric phases in the As-Zn system. The calculated values from first principles [21], which wre used as experimental inputs for the assessment, are also marked on the plot.

As-Ga-Zn ternary system:. To the best of our knowledge, there is no previous CALPHAD modeling of the As-Ga-Zn ternary system. In this work, we extrapolated the ternary phase digram from the sub-binaries As-Ga [9], Ga-Zn [10] and As-Zn (this work) using the Muggianu extrapolation method. The calculated diagram was compared to the available experimental data [2, 3, 4, 6]. The extrapolated phase diagram was in fairly good agreement with the experimental data and only slightly off in the calculated temperatures. Therefore, the description of the

Table 3: Gibbs energy functions and interaction parameters of the As-Ga-Zn ternary system. $^0G_x^\theta$ Gibbs energies are taken from the SGTE unary database [30]. The energy values are in J/mole.

Phase	Gibbs energy/Thermodynamic parameters	Ref.
Liquid	$^0G_{As_2Zn_3} = -8060 - 5.69\,T + 0.4\,G_{As}^{Liq} + 0.6\,G_{Zn}^{Liq}$	This work
	$^0L_{As,As_2Zn_3} = -22550 + 17.6\,T$	This work
	$^1L_{As,As_2Zn_3} = 911 + 5.66\,T$	This work
	$^2L_{As,As_2Zn_3} = 5785$	This work
	$^0L_{As_2Zn_3,Zn} = 36800 - 19.3\,T$	This work
	$^0L_{As,Ga} = -25503.6 - 4.3109\,T$	[9]
	$^1L_{As,Ga} = -5174.7$	[9]
	$^0L_{Ga,Zn} = 3662.8 + 27.28629\,T - 4.2\,T\,\ln(T)$	[10]
	$^1L_{Ga,Zn} = -464.2$	[10]
	$^0L_{As,As_2Zn_3,Ga} = 19500$	This work
	$^0L_{As_2Zn_3,Ga,Zn} = 17900$	This work
Rhombohedral-A7	$^0L_{As,Zn} = 25000$	This work
Zn-hcp (Zn,As)	$^0L_{As,Ga} = 25000$	This work
	$^0L_{As,Zn} = 25000$	This work
	$^0L_{Ga,Zn} = 10744$	[10]
GaAs	$G_{Ga:As} = -52176 + 132.71628\,T - 24.340629\,T\ln(T) - 5.579 \times 10^{-4}\,T^2 + 63835\,T^{-1} - 3.5689 \times 10^{-7}\,T^3$	[9]
As$_2$Zn	$G_{As:As} = 38.3\,T + 3G_{As}^{SER}$	This work
	$G_{As:Zn} = -44870 - 1.765\,T + 2G_{As}^{SER} + G_{Zn}^{SER}$	This work
α'-As$_2$Zn$_3$	$G_{As:Zn} = -7250 - 12.047\,T + 0.4G_{As}^{SER} + 0.6G_{Zn}^{SER}$	This work
α-As$_2$Zn$_3$	$G_{As:Zn} = -13700 + 1.896\,T + 0.4G_{As}^{SER} + 0.6G_{Zn}^{SER}$	This work
β-As$_2$Zn$_3$	$G_{As:Zn} = -4540 - 14.98\,T + 0.4G_{As}^{SER} + 0.6G_{Zn}^{SER}$	This work

liquid phase was optimized by adding two interaction parameters to obtain a better fit to the measured data. There is no data on the solubility of gallium in zinc arsenide compounds and according to Tuck [22], the solubility of zinc in GaAs is less than 1 at.%Zn. Thus, no solubility of the third element in the binary phases is taken into account.

The liquidus projection of the As-Ga-Zn system is shown in Fig. 2. There are six regions of primary crystallization: (As), (Ga), hcp, GaAs, As$_2$Zn$_3$ and As$_2$Zn. This ternary system consists of three congruently melting binary compounds and there are only eutectic reactions in the constituting binaries.

The measured liquidus temperatures along the GaAs-As$_2$Zn cut by Köster and Ulrich [2], the GaAs-Zn cut by Panish [3] and the GaAs-As$_2$Zn$_3$ cut by Panish [4] are superimposed on the liquidus projection diagram (Fig. 2). There is a very good agreement between the measured and the calculated values.

The schematic of the monovariant and invariant reactions of the As-Ga-Zn ternary system is illustrated in Fig. 3. For the quasi-binary eutectic reactions (marked by 'e'), the maximum temperature is mentioned. There are three ternary eutectic reactions (marked by 'E') and one ternary peritectic reaction (marked by 'P') in this system.

Three isoplethal sections of the As-Ga-Zn ternary system along GaAs-Zn, GaAs-As$_2$Zn$_3$ and GaAs-As$_2$Zn cuts are shown in Fig. 4a to c, respectively. In agreement with Panish [3] and Pelevin et al. [6], along the GaAs-Zn cut three primary fields appear upon crystallization: GaAs (0-71.0 at.%Zn), As$_2$Zn$_3$ (71.0-~100 at.%Zn) and Zn (at about 100 at.%Zn). Our calculation shows that there is only one thermal event (polymorphic transformation $\beta \rightarrow \alpha'$) at the temperature range 883-918 K, similar to that predicted by Panish [3]. However, Pelevin et al. [6] have registered two thermal effects at this temperature range.

Moreover, according to both [3] and [6], As$_2$Zn$_3$ should precipitate along the GaAs-Zn cut at a slightly lower Zn composition and in a wider temperature range, while our calculation contradicts that. For instance, in both studies, at the composition of 68 at.%Zn, 16 at.%As, 16 at.%Ga (marked with the dashed line in Fig. 4a), As$_2$Zn$_3$ was the first solid phase reported to form on crystallization. We compare the Scheil solidification simulations of 68 at.% Zn composition along GaAs-Zn cut and along the As-rich and As-poor sides of this cut (with the same zinc composition) in Fig 4-d. In a Scheil solidification simulation which utilizes a non-equilibrium condition, it is assumed that the solid phases are frozen and the diffusion occurs only in the liquid phase. Clearly, in the As-rich side of the GaAs-Zn cut (line 1), As$_2$Zn$_3$ is the first solid phase to form but on the As-poor side (line 3), GaAs forms first. To compare
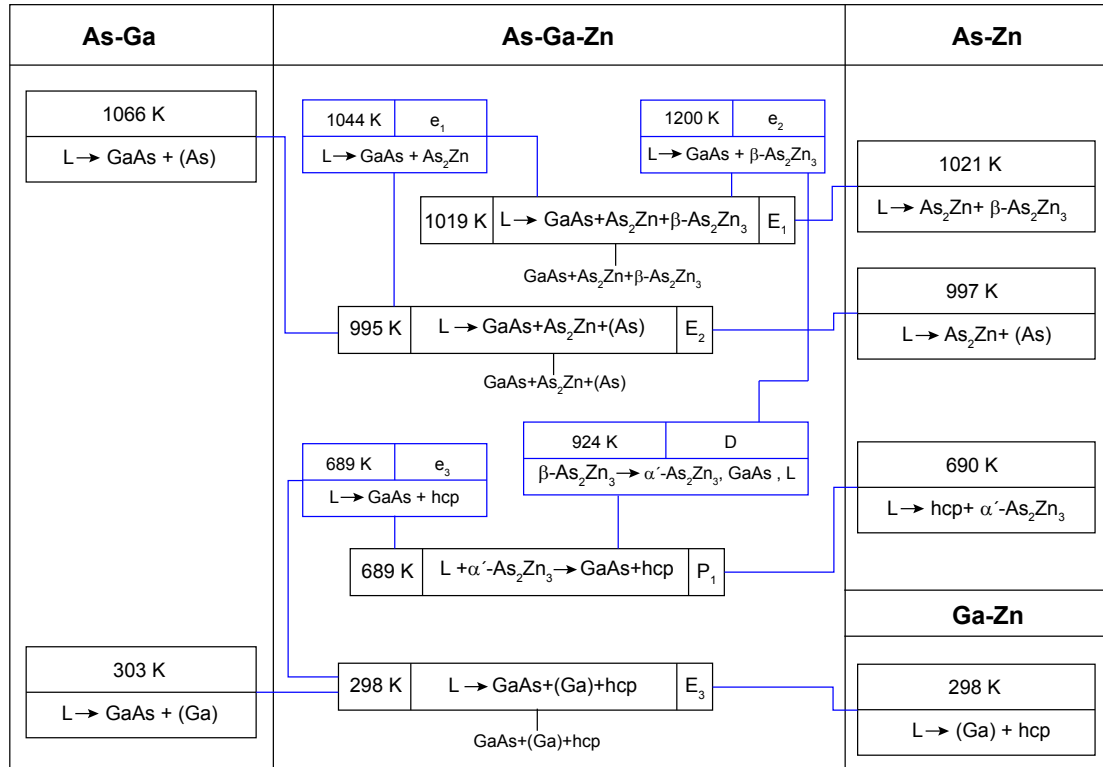
As-Ga | **As-Ga-Zn** | **As-Zn**

| 1066 K |
| L → GaAs + (As) |

| 1044 K | e₁ |
| L → GaAs + As₂Zn |

| 1200 K | e₂ |
| L → GaAs + β-As₂Zn₃ |

| 1019 K | L → GaAs+As₂Zn+β-As₂Zn₃ | E₁ |

GaAs+As₂Zn+β-As₂Zn₃

| 1021 K |
| L → As₂Zn+ β-As₂Zn₃ |

| 995 K | L → GaAs+As₂Zn+(As) | E₂ |

GaAs+As₂Zn+(As)

| 997 K |
| L → As₂Zn+ (As) |

| 924 K | D |
| β-As₂Zn₃→ α´-As₂Zn₃, GaAs , L |

| 689 K | e₃ |
| L→ GaAs + hcp |

| 690 K |
| L → hcp+ α´-As₂Zn₃ |

| 689 K | L +α´-As₂Zn₃→ GaAs+hcp | P₁ |

Ga-Zn

| 303 K |
| L → GaAs + (Ga) |

| 298 K | L → GaAs+(Ga)+hcp | E₃ |

GaAs+(Ga)+hcp

| 298 K |
| L → (Ga) + hcp |

Figure 3: The schematic of the invariant reactions with the liquid phase in the As-Ga-Zn system. 'E', 'P', 'D' and 'e' stand for ternary eutectic, ternary peritectic, degenerate and quasi-binary eutectic reaction types, respectively.

with the equilibrium condition, the isopleths along the As-rich ($x_{As} − x_{Ga} = 0.2$) and As-poor ($x_{Ga} − x_{As} = 0.2$) sides of the GaAs-Zn cut are calculated (see Fig. A.6 in Supplementary Information). These isopleths also confirm the precipitation of As₂Zn₃ as the first solid phase at the composition of 68 at.%Zn at the As-rich side of the GaAs-Zn cut.

The GaAs-As₂Zn₃ vertical section is shown in Figure 4-b and the experimental data of Köster and Ulrich [2] and Panish [4] are superimposed on the diagrams. The calculated and the measured temperatures of the first and the second thermal events are in agreement. However, the third thermal event at around 1000 K which should be the temperature of the reaction E₁ according to [4] does not occur exactly along this cut. The Scheil solidification simulation (not shown here) shows that this reaction occurs at the As-rich side of this cut.

The third calculated vertical section, GaAs-As₂Zn, is shown in Figure 4-c. The experimental temperatures measured by Köster and Ulrich [2] are compared to the calculated values. The first thermal effect is the surface of the liquidus, the second one is the quasi-binary eutectic reaction between GaAs and As₂Zn.

Summary. We have thermodynamically assessed the As-Zn and As-Ga-Zn systems using the CALPHAD method, taking the available first principles and experimental data into account. A set of self-consistent parameters are optimized and presented in this work. We have compared the calculated As-Zn binary phase diagram and isoplethal sections and liquidus projection of the As-Ga-Zn ternary phase diagram with experimental data from the literature. There is a very good agreement between the experimental and calculated values.

References

[1] L. C. Keizer, X. Tang, R. Z. C. van Meerten, and L.J. Giling. Doping of gallium arsenide in MOCVD: Equilibrium calculations. *J. Crys. Growth*, 102(3):667 – 677, 1990.

[2] W. Köster and W. Ulrich. Das dreistoffsystem gallium-arsen-zink. *Z. Metallkd.*, 49:361 – 364, 1958.

[3] M. B. Panish. The gallium-arsenic-zinc system. *J. Phys. Chem. Solids*, 27:291 – 298, 1966.

[4] M. B. Panish. The As-rich region of the Ga-As-Zn ternary phase system-Modification of the ternary diagram. *J. Electrochem. Soc.*, 113:861, 1966.

[5] K. K. Shih, J. W. Allen, and G. L. Pearson. Gas phase equilibria in the system Ga-As-Zn. *J. Phys. Chem. Solids*, 29(2):367 – 377, 1968.

[6] O. V. Pelevin, F. A. Gimel'farb, M. G. Miltvidskii, and B. P. Zherdev. The polythermal cross section GaAs-Zn. *Inorg. Mater.*, 8:919 – 923, 1972.

[7] A. S. Jordan. The liquidus surfaces of ternary systems involving compound semiconductors: II. Calculation of the liquidus isotherms and component partial pressures in the Ga-As-Zn and Ga-P-Zn systems. *Metall. Trans.*, 2(7):1965 – 1970, 1971.

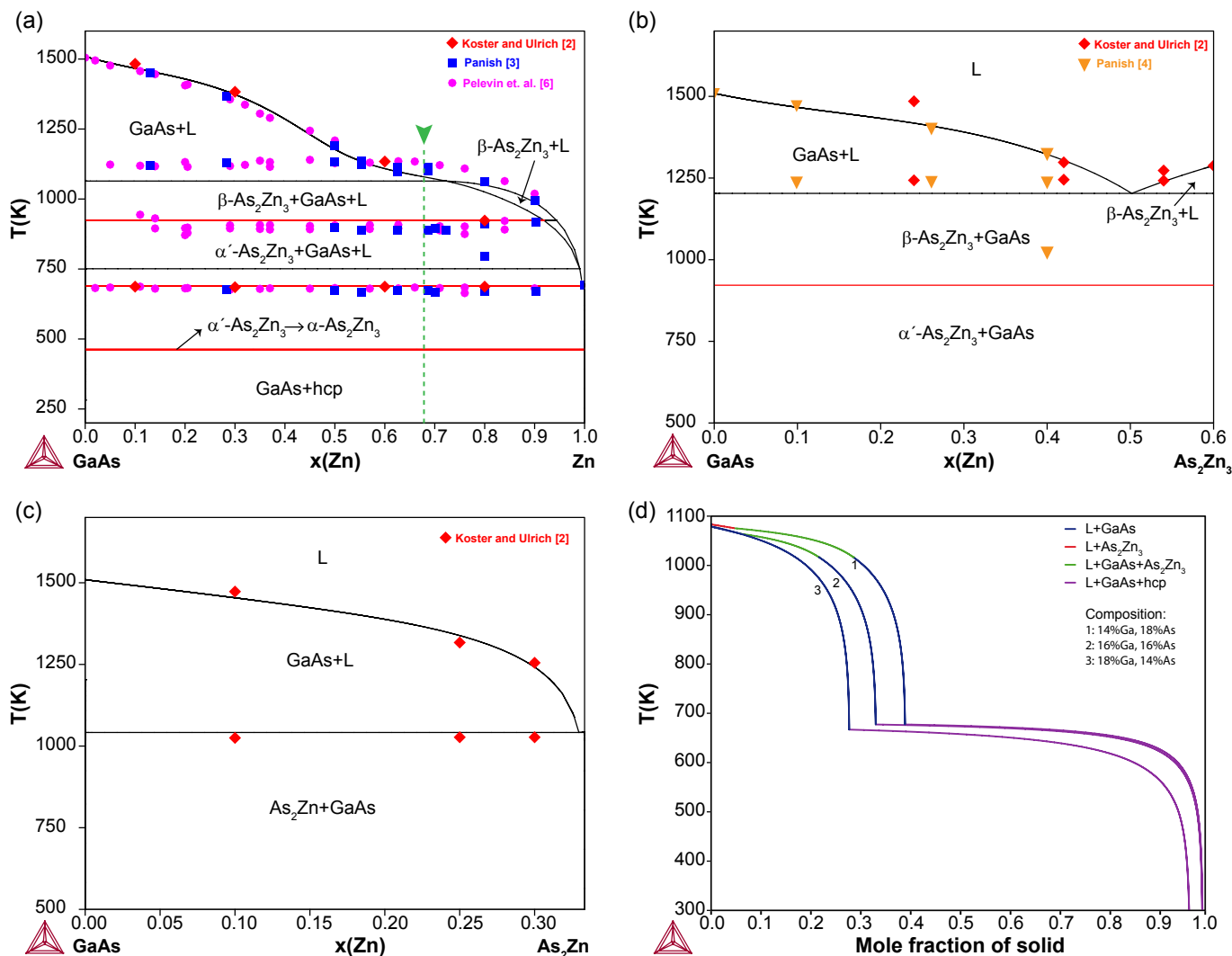[8] L. Kaufman and H. Bernstein. *Computer Calculations of Phase Diagrams*. New York: Academic Press, 1970.

Figure 4: (a) GaAs-Zn, (b) GaAs-As$_2$Zn$_3$ and (c) GaAs-As$_2$Zn isoplethal sections of the As-Ga-Zn phase diagram. The experimental data are superimposed on the diagrams by symbols: diamond [2], square [3], triangle [4] and circle [6]. (d) Scheil solidification simulations of the 68 at.% Zn composition along the GaAs-Zn cut (line 2), As-rich (line 1) and As-poor (line 3) side of the same cut.

[9] I. Ansara, C. Chatillon, H. L. Lukas, T. Nishizawa, H. Ohtani, K. Ishida, M. Hillert, B. Sundman, B. B. Argent, A. Watson, T. G. Chart, and T. Anderson. A binary database for III-V compound semiconductor systems. *Calphad*, 18(2):177 – 222, 1994.

[10] J. Dutkiewicz, Z. Moser, L. Zabdyr, D. D. Gohil, T. G. Chart, I. Ansara, and C. Girard. The Ga-Zn (Gallium-Zinc) system. *Bull Alloy Phase Diagr.*, 11(1):77–82, 1990.

[11] C. Chatillon, I. Ansara, A. Watson, and B. B. Argent. Re-assessment of the thermodynamic properties and phase diagrams of the Ga-As and In-As systems. *Calphad*, 14(2):203 – 214, 1990.

[12] H. Okamoto. The As-Zn (arsenic-zinc) system. *J. Phase Equilib.*, 13(2):155–161, 1992.

[13] V. Lazarev, S. F. Marenkin, S. I. Maksimova, B. Hkuseinov, and V. Ya. Shevchenko. The region of homogenity of ZnAs$_2$. *Izv.Akad.Nauk SSSR, Neorg. Mater.*, 15:586–587, 1979.

[14] W. Heike. Mitteilungen aus dem metallographischen institut der bergakademie freiberg. das erstarrungsbild der zink-arsen-legierungen. *Z. Anorg. Allg. Chem.*, 118:264–268, 1921.

[15] J. H. Greenberg, V. N. Guskov, V. B. Lazarev, and A. A. Kotliar. Solid state phase transition in Zn$_3$As$_2$. *Mater. Res. Bull.*, 17(10):1329 – 1335, 1982.

[16] V. B. Lazarev, V. N. Guskov, and J. H. Greenberg. P-T-X phase equilibria

in the system Zn-As. *Materials Research Bulletin*, 16(9):1113 – 1120, 1981.

[17] K. Friedrich and A. Leroux. Zinc and Arsenic. *Metallurgie*, 3:477–479 (in German), 1906.

[18] K. Yamaguchi, A. Mikula, K. L. Komarek, and K. Itagaki. Thermodynamic investigations of the liquid As-Zn and As-Cd systems by drop calorimetry. *Z. Metallkd.*, 82:591–598, 1991.

[19] V. J. Lyons. The dissociation pressure of ZnAs$_2$. *J.Phys. Chem.*, 63(7):1142–1144, 1959.

[20] R. C. Schoonmaker and K. J. Lemmerman. Vaporization of Zn$_3$As$_2$. *J. Chem. Eng. Data*, 17:139 – 143, 1972.

[21] Materials Project. http://www.materialsproject.org.

[22] B. Tuck. The GaAs/Zn solidus at 1000 °C. *J. Phys. D: Appl. Phys.*, 9:2061 – 2073, 1976.

[23] D. Schiferl and C. S. Barrett. The crystal structure of Arsenic at 4.2, 78 and 299 K. *J. Appl. Crystallogr.*, 2:30–36, 1969.

[24] B. D. Sharma and J. A. Donohue. A refinement of the crystal structure of gallium. *Z. Kristallogr.*, 117:293 – 300, 1962.

[25] D. A. Davies and E. A. Owen. An X-ray investigation on the solid solutions of certain elements in zinc. *Br. J. Appl. Phys.*, 15:1309 – 1314, 1964.

[26] M. E. Straumanis and C. D. Kim. Phase extent of gallium arsenide de-

termined by the lattice constant and density method. *Acta Crystallogr.*, 19:256 – 259, 1965.

[27] M. E. Fleet. The crystal structure of $ZnAs_2$. *Acta CrysActa Cr. B*, 30:122–126, 1974.

[28] C. W. F. T. Pistorius. Melting and polymorphism of Cs_3As_2 and Zn_3As_2 at high pressures. *High Temp. High Press.*, 7:441–449, 1975.

[29] S. Weglovski and K. Lukaszewicz. Phase transitions of Cd_3As_2 and Zn_3As_2. *Bull. Acad. Pol. Sci., Ser. Sci. Chim*, 16:177–182, 1968.

[30] SGTE unary database ver. 4.4. *Updated from: A. T. Dinsdale, Calphad 15, 1991,317*.

[31] I. Ansara, A. Dinsdale, and M. Rand, editors. *COST 507 Definition of Thermochemical and Thermophysical Properties to Provide a Database for the Development of New Light Alloys*. Office for Official Publications of the European Communities, 1998.

[32] R. Schmid-Fetzer and B. Hallstedt. Is zinc HCP-Zn or HCP-A3? *Calphad*, 37:34–36, 2012.

[33] B. Sundman, B. Jansson, and J. O. Andersson. The Thermo-Calc databank system. *Calphad*, 9(2):153 – 190, 1985.

[34] H. L. Lukas, S. G. Fries, and B. Sundman. *Computational Thermodynamics: The Calphad Method*. Cambridge Uni. press, 2007.

[35] R. Schmid-Fetzer, D. Andersson, P. Y. Chevalier, L. Eleno, O. Fabrichnaya, U. R. Kattner, B. Sundman, C. Wang, A. Watson, L. Zabdyr, and M. Zinkevich. Assessment techniques, database design and software facilities for thermodynamics and diffusion. *Calphad*, 31(1):38–52, 2007.

[36] J. O. Andersson, T. Helander, L. Höglund, P. Shi, and B. Sundman. Thermo-Calc & DICTRA, computational tools for materials science. *Calphad*, 26(2):273–312, 2002.

Thermodynamic Assessment of As-Zn and As-Ga-Zn Systems

Masoomeh Ghasemi[*] and Jonas Johansson

Solid State Physics, Lund University,Lund, Sweden
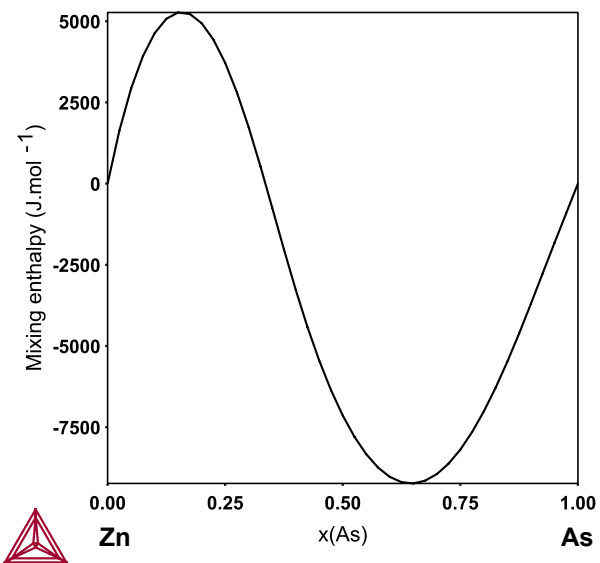
[*] masoomeh.ghasemi@ftf.lth.se

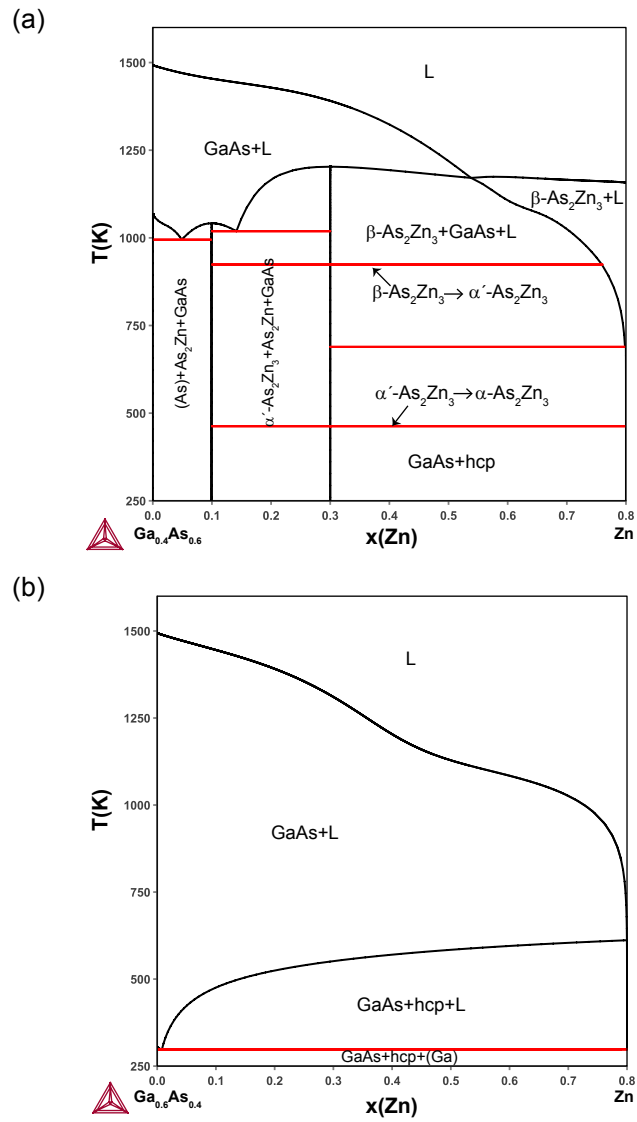Figure A.5: Calculated mixing enthalpy of As-Zn liquid alloys at 1300 K.

Figure A.6: The isopleths along (a) x(As)-x(Ga)=0.2 and (b) x(Ga)-x(As)=0.2 sections of the As-Ga-Zn ternary phase diagram.